Journal of Alloys and Compounds 511 (2012) 195–197

Contents lists available at SciVerse ScienceDirect

Journal of Alloys and Compounds

journal homepage: www.elsevier.com/locate/jallcom

Synthesis of aligned copper oxide nanorod arrays by a seed mediated hydrothermal method

Liqing Liu, Kunquan Hong*, Tengteng Hu, Mingxiang Xu

Department of Physics, Southeast University, Nanjing 211189, PR China

ARTICLE INFO

Article history:
Received 11 July 2011
Received in revised form 8 September 2011
Accepted 9 September 2011
Available online 16 September 2011

Keywords:
Nanomaterials
Seed crystals
Semiconducting materials

ABSTRACT

The synthesis of ordered copper oxide (CuO) nanorod arrays has been obtained using a seed-mediated hydrothermal method. Aligned CuO nanorods were obtained on fluorine doped tin oxide glass substrates over a large scale at low temperature ranging from 75 to 85 °C. It is found the CuO nanoseeds play an important role to facilitate the growth of those aligned CuO nanorods. The band gap energy of the CuO nanorods was estimated by ultraviolet–visible absorption spectroscopy. The growth mechanism of this method was also investigated.

1. Introduction

As a p-type semiconducting material with band-gap of 1.2 eV, copper oxide (CuO) has been widely used in various applications, such as dye-sensitized solar cells [1], heterogeneous catalyst [2], gas sensors [3] and lithium–copper oxide electrochemical cells [4], etc. CuO is also renowned for its central function in cupric based high T_c superconductors [5], in which its Cu valence electrons and their spin fluctuation dominate the characteristics of superconductivity. CuO nanostructures are expected to improve the performance of these devices as well as to open up new applications. Therefore, the fabrication of nanostructured CuO shows significant importance both in terms of fundamental studies and commercial applications. Recently, various CuO nanostructures, such as nanowires [6], nanotubes [7], nanoribbons [8] and nanoplates [9], have been successfully synthesized by various techniques, including thermal oxidization of Cu foil [10], hydrothermal method [11,12], templating method [13], microwave-assisted hydrothermal synthesis method [14,15], and electrospinning [16], etc. Any methods that can yield production of large-area CuO nanorod arrays, of course at an acceptable cost, are welcome to facilitate the realistic applications of CuO nanorods. However few studies have been reported on the synthesis of well aligned CuO nanorod arrays on the conducting glass substrate at a large scale, with low temperature and easily adoptable. In this paper, the strategy for obtaining well aligned and large scale CuO nanorod arrays on the conducting glass will be discussed. We used a seed-mediated growth method [17–19] to fabricate vertically aligned CuO nanorods on fluorine doped tin oxide (FTO) glass at low temperature of 75–80 °C by using a hydrothermal method. It is found that coating the substrate with a layer of CuO nanoseeds is favorable for the growth of those aligned CuO nanorods.

2. Experimental details

Synthesis of CuO nanorods was carried out by using a CuO nanoseed-mediated growth method. In a typical process, CuO nanoseed particles were first grown on FTO glass via an alcohothermal method [20]. Specifically, a clean FTO glass substrate (2 cm × 3 cm) was wetted with a 10 mM ethanolic solution of copper acetate monohydrate ($Cu(CH_3COO)_2{\cdot}H_2O$) for 10 s. After dried in air, this substrate was annealed at 100 °C for 1 min to enhance the adhesion. Then the substrate was annealed at 250 °C for 2.5 h to obtain the CuO nanoseeds layer. Aligned CuO nanorod arrays were prepared by dipping this substrate 5 cm under the solution of a mixture of equimolar 25 mM copper nitrate trihydrate ($Cu(NO_3)_2{\cdot}3H_2O$) and hexamethylenetetramine (HMTA, $C_6H_{12}N_4$) in deionized (DI) water and being heated with an electric-heated water bath. This heating process was performed for 2–5 h with different growth temperature varied from 70 to 85 °C. Then the substrate was taken out from the growth solution. A homogeneous red brown layer was observed full of the surface of FTO glasses. The samples were rinsed with DI water softly several times and dried in air flow.

The morphology of the CuO nanorods was evaluated by field emission scanning electron microscopy (FESEM, JSM-7000F, JEOL). The crystal structure of the CuO nanorods was inspected by X-ray diffractometer (Rigaku D8) with Cu Kα radiation (λ = 0.15406 nm). Data acquisition was accomplished for 2θ values varied from 20° to 80° at a step length of 0.02°. The UV–visible (UV–vis) absorption spectrum of the products was recorded by a UV–Vis spectrophotometer (Shimadzu UV2450).

3. Results and discussion

Three samples were selected as the typical results in this work, which were grown at temperature of 85, 80 and 75 °C for 4 h for

* Corresponding author. Tel.: +86 25 52090606 8401; fax: +86 25 52090606 8203.
E-mail addresses: hongkq@gmail.com (K. Hong), mxxu@seu.edu.cn (M. Xu).

0925-8388/$ – see front matter © 2011 Elsevier B.V. All rights reserved.
doi:10.1016/j.jallcom.2011.09.028

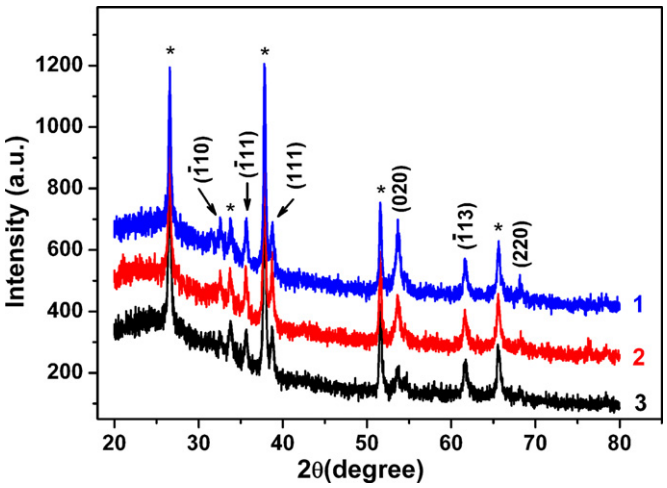

Fig. 1. XRD spectra of CuO nanorods grown on FTO glass substrates at temperature 85, 80 and 75 °C for 4 h for samples #1, #2 and #3, respectively.

samples #1, #2 and #3, respectively. The structure and the phase of the CuO nanostructures were characterized by using XRD technique. Fig. 1 shows the typical XRD spectra of the CuO nanorods for samples #1, #2 and #3 respectively. It is found the XRD spectra of the three samples are almost the same as each other, which indicates the grown CuO nanorods have the similar crystal structures. The strongest peaks marked as asterisks are corresponding to the crystal structures of SnO_2, which come from the substrate of FTO glasses. For the peaks corresponded to CuO, six peaks at 32.54°, 35.56°, 38.75°, 53.56°, 63.84° and 68.12° respectively, are clearly recognized (Fig. 1), which can be well indexed to the monoclinic-phase CuO, with lattice parameters $a = 0.689$ nm, $b = 0.3420$ nm, $c = 5.130$ nm and $\beta = 99.57°$ (JCPDS Card No. 89-5899). The relatively weak peaks compared with those from the substrate are possibly due to the low growth temperature adopted. The broad Bragg peaks of CuO in the current measurement could be related to small crystallite size of the nanorods. No characteristic peaks from impurities, such as $Cu(OH)_2$ or Cu_2O, can be obviously observed. EDX data shows the molar ratio of Cu and O is 1:1.04, which is consistent with the chemical composition of CuO, indicating high purity of those CuO nanorods.

Fig. 2(a)–(c) shows the side view FESEM images of the typical CuO nanorod arrays growing on FTO glass substrates. From Fig. 2(a)–(c), two layers are clearly observed. The bottom dense layer is the CuO nanoseeds, with thickness of about 300 nm. On the nanoseeds layer, while the entire substrate surface is covered by vertically aligned CuO nanorods. The detail morphology of the samples shows these nanorods are not uniform along the length. They have tapered tips with smaller diameters. Inset of Fig. 2(c) shows the top view of sample #3, in which the tapered tips can be clearly observed.

It is reported that several parameters affect the size and shape of CuO nanorods grown from solution, such as temperature, molar ratio of Cu^{2+} and OH^-, reaction time and concentration of the solution [21–23], etc. Especially the morphologies of CuO nanorods are dramatically affected by the growth temperature. From the SEM images of the samples synthesized with the same method except adjusting the growth temperatures (Fig. 2(a)–(c)), it is found the average diameter of nanorods decreases with the growth temperature. The average diameter of these nanorods was about 56 nm for growing at 85 °C, while larger diameter nanorods were obtained with lower heating temperature. For example, the average diameters were 60 and 73 nm when growing at 80 °C and 75 °C, respectively. The mechanism of this dependence of size on growth temperature may be explained as following. When heated in solution, HMTA will be decomposed to produce ammonia [24], which then further hydrolyzes to provide OH^-. The OH^- ion will react with copper nitrate to produce the insoluble copper hydroxides. The concentration of OH^- will increase with growth temperature for fast decomposition speed of HMTA in high temperature. Then more insoluble copper hydroxides are formed. This will increase the supersaturation ratio of the insoluble copper hydroxides, facilitating the formation of smaller nanorods with higher density according to the nucleation theory [25,26]. To reveal the role of the seeds for the CuO nanorods growth, samples were also prepared using the same method and conditions as above except that the nanoseeds were omitted. No nanorod was observed if there was no such seed layer. Contrarily, if the nanoseed layer presented, CuO nanorods can also grow on other solid supports by the same

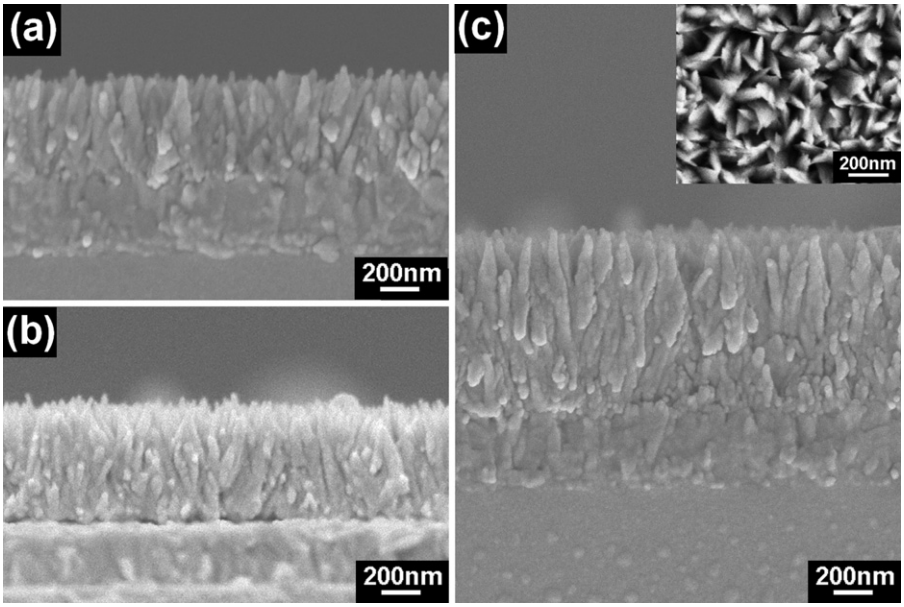

Fig. 2. SEM images of CuO nanorod arrays on FTO glass substrates for samples #1 (a), #2 (b) and #3 (c) respectively. The top morphology of sample #3 is shown as the inset of (c).

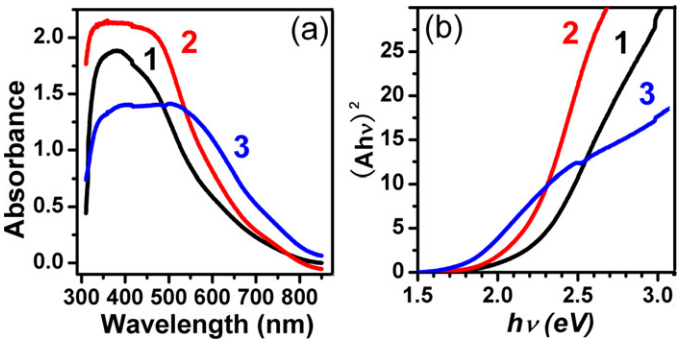

Fig. 3. UV–vis optical absorption spectra with 4 h for samples #1–3 on FTO glass substrates (a), and the $(Rh\nu)^2$ as a function of $h\nu$ (b) according to the data from (a).

method, such as silicon wafer and micro microscope slide, etc. As seen in Fig. 2(c), small oriented nanocrystals are formed in the seed layer. These nanocrystals can produce the necessary nucleated sites for the nanorods growing afterwards. The thickness of the seed layer also effects on the final morphologies. Relative thin seed layer is preferred. To ensure the orientation and uniformity of the seed film, here seed layer with thickness of 50–300 nm is adopted in this work. When using thick seed layer, these nanocrystals are randomly orientated or form big crystals, thus retarding the nanorods growth.

For the determination of the band gap, UV–vis absorption spectra of the CuO nanorod arrays of samples #1–3 are shown as curves 1–3 in Fig. 3(a), respectively. The absorption peaks are centered at 378, 398 and 439 nm for samples #1–3. The frequency dependence of the absorption coefficient of semiconductors is given by: $Ah\nu = a(h\nu - E_g)^n$, where A is the absorption coefficient, ν is the frequency of photons, a is a proportionality constant, $n = 1/2$ for direct transitions and $n = 2$ for indirect transitions [27–29]. The $(Ah\nu)^2$ as a function of $h\nu$ in Fig. 3(b) has plotted according to the data from Fig. 3(a). The curves in the visible range can be linearly fitted, indicating that the absorption edge is due to a direct allowed transition [19]. According to the prolongation of linear section, the optical band gap energy is calculated to be 2.2, 2.1, and 1.8 eV for samples #1, #2, and #3, respectively (Fig. 3(b)). These values are larger than the reported value of bulk CuO (1.2 eV) due to quantum confinement effects [30]. The band gap of the CuO nanorods grown at high temperature is larger than that of the sample grown at lower temperature due to large size confinement effects caused by their relatively smaller diameter. The optical absorption spectra shift toward higher energy with decrease in size of the nanorods.

4. Conclusions

In this paper, we presented a simple seed-mediated approach for growing large-scale, uniform vertically oriented CuO nanorods on FTO glass substrates by hydrothermal method. The size of the substrate is only limited by the growth chamber. The UV–vis spectra show these CuO nanorods have band gaps of 2.2, 2.1, and 1.8 eV for growth at 85, 80, and 75 °C, respectively. Therefore, this method can produce aligned CuO nanorods at a large scale at low temperature, which is useful for the application of CuO nanorods and helpful to grow nanorod arrays of other materials.

Acknowledgments

This work was supported by National Science Foundation of China (NSFC Grant Nos. 10804017 and 11047123), Natural Science Foundation of Jiangsu Province of China (Grant No. BK2010421), and Foundation for Climax Talents Plan in Six-Big Fields of Jiangsu Province of China (Grant No. 1107020070).

References

[1] Y. Liu, L. Liao, J. Li, C. Pan, J. Phys. Chem. C 111 (2007) 5050–5056.
[2] J.B. Reitz, E.I. Solomon, J. Am. Chem. Soc. 120 (1998) 11467–11478.
[3] A. Chowdhuri, V. Gupta, K. Sreenivas, Appl. Phys. Lett. 84 (2004) 1180–1182.
[4] G.F. Zou, H. Li, D.W. Zhang, K. Xiong, C. Dong, Y.T. Qian, J. Phys. Chem. B 110 (2006) 1632–1637.
[5] J.G. Bednorz, K.A. Muller, Z. Phys. B 64 (1986) 189–193.
[6] Q. Liu, Y.Y. Liang, H.J. Liu, J.M. Hong, Z. Xu, Mater. Chem. Phys. 98 (2006) 519–522.
[7] M. Cao, C. Hu, Y. Wang, Y. Guo, C. Guo, E. Wang, Chem. Commun. 15 (2003) 1884–1885.
[8] H.W. Hou, Y. Xie, Q. Li, Cryst. Growth Des. 5 (2005) 201–205.
[9] K.B. Zhou, R.P. Wang, B.Q. Xu, Y.D. Li, Nanotechnology 17 (2006) 3939–3943.
[10] X.C. Jiang, T. Herricks, Y.N. Xia, Nano Lett. 2 (2002) 1333–1338.
[11] M. Abaker, A. Umar, S. Baskoutas, S.H. Kim, S.W. Hwang, J. Phys. D: Appl. Phys. 44 (2011) 155405.
[12] M.H. Cao, Y.H. Wang, C.X. Guo, Y.J. Qi, C.W. Hu, E.B. Wang, J. Nanosci. Nanotechnol. 4 (2004) 824–828.
[13] S.L. Wang, H. Xu, L.Q. Qian, X. Jia, J.W. Wang, Y.Y. Liu, W.H. Tang, et al., J. Solid State Chem. 182 (2009) 1088–1093.
[14] D.P. Volanti, M.O. Orlandi, J. Andrés, E. Longo, CrystEngComm 12 (2010) 1696–1699.
[15] I. Bilecka, M. Niederberger, Nanoscale 2 (2010) 1358–1374.
[16] H. Wu, D.D. Lin, W. Pan, Appl. Phys. Lett. 89 (2006) 133125.
[17] H.E. Unalan, P. Hiralal, N. Rupesinghe, S. Dalal, W.I. Milne, G.A.J. Amaratunga, Nanotechnology 19 (2008) 255608.
[18] A.A. Umar, M. Oyama, Cryst. Growth Des. 7 (2007) 2404–2409.
[19] X.Y. Hou, J. Feng, X.D. Xu, M.L. Zhang, J. Alloys Compd. 491 (2010) 258–263.
[20] Z.S. Hong, Y. Cao, J.F. Deng, Mater. Lett. 52 (2002) 34–38.
[21] R.J. Wu, Z.Y. Ma, Z.G. Gu, Y. Yang, J. Alloys Compd. 504 (2010) 45–49.
[22] Y.J. Zhang, S.W. Or, X.L. Wang, T.Y. Cui, W.B. Cui, Y. Zhang, Z.D. Zhang, Eur. J. Inorg. Chem. (2009) 168–173.
[23] Y.G. Zhang, S.T. Wang, X.B. Li, L.Y. Chen, Y.T. Qian, Z.D. Zhang, J. Cryst. Growth 291 (2006) 196–201.
[24] Z.Z. Zhou, Y.L. Deng, J. Phys. Chem. C 113 (2009) 19853–19858.
[25] J.A. Dirksen, T.A. Ring, Chem. Eng. Sci. 46 (1991) 2389–2427.
[26] Q.C. Li, V. Kumar, Y. Li, H.T. Zhang, T.J. Marks, R.P.H. Chang, Chem. Mater. 17 (2005) 1001–1006.
[27] S. Tsunekawa, T. Fukuda, A. Kasuya, J. Appl. Phys. 87 (2000) 1318.
[28] T. Maruyama, Sol. Energy Mater. Sol. Cells 56 (1998) 85–92.
[29] K. Manmeet, K.P. Muthe, S.K. Despande, S. Choudhury, J.B. Singh, N. Verma, S.K. Gupta, J.V. Yakhmi, et al., J. Cryst. Growth 289 (2006) 670–675.
[30] K. Borgohain, S. Mahamuni, J. Mater. Res. 17 (2002) 1220.